

Expanded Metabolic Reconstruction of *Helicobacter pylori* (iT341 GSM/GPR): an In Silico Genome-Scale Characterization of Single- and Double-Deletion Mutants

Ines Thiele,[†] Thuy D. Vo,[†] Nathan D. Price, and Bernhard Ø. Palsson*

Department of Bioengineering, University of California, San Diego, California

Received 14 December 2004/Accepted 19 April 2005

Helicobacter pylori is a human gastric pathogen infecting almost half of the world population. Herein, we present an updated version of the metabolic reconstruction of *H. pylori* strain 26695 based on the revised genome annotation and new experimental data. This reconstruction, iT341 GSM/GPR, represents a detailed review of the current literature about *H. pylori* as it integrates biochemical and genomic data in a comprehensive framework. In total, it accounts for 341 metabolic genes, 476 intracellular reactions, 78 exchange reactions, and 485 metabolites. Novel features of iT341 GSM/GPR include (i) gene-protein-reaction associations, (ii) elementally and charge-balanced reactions, (iii) more accurate descriptions of isoprenoid and lipopolysaccharide metabolism, and (iv) quantitative assessments of the supporting data for each reaction. This metabolic reconstruction was used to carry out in silico deletion studies to identify essential and conditionally essential genes in *H. pylori*. A total of 128 essential and 75 conditionally essential metabolic genes were identified. Predicted growth phenotypes of single knockouts were validated using published experimental data. In addition, in silico double-deletion studies identified a total of 47 synthetic lethal mutants involving 67 different metabolic genes in rich medium.

Helicobacter pylori is a human pathogen that is often associated with gastric inflammation and peptic ulcer disease (33). Interests in studying this bacterium and its role in these diseases are reflected by numerous biochemical and genetic studies (14, 23, 27–32, 36) and the sequenced genome (44). In an effort to integrate and reconcile these multiple data sources, an initial genome-scale metabolic network of this bacterium was reconstructed 2 years ago (39). Since then, many new studies, including a revised genome annotation (1), have been reported and have significantly enhanced the understanding of this pathogen. In order to account for these new data and to improve the quality of the model, we present here an updated and expanded reconstruction of the *H. pylori* 26695 metabolic network, referred to as iT341 GSM/GPR. This name was based on the convention introduced by Reed et al. (37), where the letter “i” refers to an in silico strain, “IT” is the initial of the principal author of the reconstruction, and “341” is the number of genes included in the reconstruction. Also, GSM stands for genome-scale model, and GPR stands for gene-protein-reaction associations (37).

In this study, every reaction was elementally and charge balanced and was assigned a confidence level. An accompanying metabolic map illustrates the connectivity among metabolites and reactions in the network (see Figure S1 in the supplemental data at <http://gcrp.ucsd.edu/organisms/hpylori.html>). This network was used to predict growth phenotypes of

single-knockout mutants. Results of these predictions were validated with published experimental data. In addition, we identified potential conditional essential double-gene-deletion mutants and enzymatic reactions that are necessary for the production of each biomass constituent.

MATERIALS AND METHODS

Constraint-based modeling. The reconstructed metabolic network was represented by a stoichiometric matrix, S ($m \times n$), where m is the number of metabolites and n is the number of reactions. Reactions within the network were mass balanced such that $S \cdot v = 0$, where v was a steady-state flux vector (9, 22). Additional constraints on each reaction had the form $\alpha_i \leq v_i \leq \beta_i$, where α_i and β_i represented the lower and upper limits, respectively, of the corresponding reaction flux. α_i was set to zero for irreversible reactions, whereas β_i was set to measured uptake rates for transport reactions or the V_{\max} of the corresponding enzymes. The unit for each reaction flux was defined to be mmol/h/g (dry weight), in agreement with the typical unit of uptake rates and reaction fluxes used for microorganisms (8, 37). The growth rate was therefore reported in units of 1/h.

Reconstruction of iT341 GSM/GPR. The previous metabolic network of *H. pylori*, here referred to as iCS291 (39), was used as a basis for the reconstruction of iT341 GSM/GPR. Each gene and its associated reaction(s) in iCS291 were carefully curated and compared to the current biochemical and genomic data. Only reactions consistent with current data were retained from the previous reconstruction. These reactions were elementally and charge balanced before being included in iT341 GSM/GPR. Reactions catalyzed by enzymes with putative gene assignments (1, 44) were also included. Reactions that did not agree with the most current data were either modified or omitted. Finally, we added reactions that were consistent with existing physiological data but for which no corresponding enzyme or loci have been found. We relied on information retrieved from the KEGG database (19, 20) for reactions gene products that have no specific biochemical characterization in *H. pylori*. The molecular formulas and charges for each metabolite in the model were determined based on a neutral intracellular pH (42). The reconstruction and functional analysis of iT341 GSM/GPR were performed using the software package SimPheny (Genomatica Inc., San Diego, CA). A comprehensive list of all compounds and reactions of the metabolic network can be found in the supplemental material (<http://gcrp.ucsd.edu/organisms/hpylori.html>).

* Corresponding author. Mailing address: Department of Bioengineering, University of California—San Diego, 9500 Gilman Dr. 0412, La Jolla, CA 92093-0412. Phone: (858) 534-5668. Fax: (858) 822-3120. E-mail: palsson@ucsd.edu.

[†] These authors contributed equally to this work.

TABLE 1. Compositions of in silico media^a

Component	Min I	Min II	Min III	Min IV	Rich medium ^a
Medium basis		Min I	Min II	Min III	Min IV
Amino acids	L-Alanine, D-alanine, L-arginine, L-histidine, L-isoleucine, L-leucine, L-methionine, L-valine		L-Asparagine, L-aspartate, L-glutamine, L-glutamate, L-serine, D-serine	L-Cysteine, L-lysine, L-phenylalanine, L-proline, L-threonine, L-tryptophane, L-tyrosine	Glycine, ornithine
Carbon sources		D-Glucose	Pyruvate, lactate, malate, fumarate, succinate, α -ketoglutarate		
Nucleotides and/or nucleosides					Adenine, cytidine, deoxyadenosine, deoxycytidine, deoxyuridine, guanine, hypoxanthine, nicotinamide D-ribonucleotide, orotate, thymidine, uracil, uridine, xanthine
Others	Phosphate, sulfate, iron (II), iron (III), pimelate, thiamine, water, oxygen, protons				Acrylamide, acetate, acetoacetate, acetaldehyde, acetamide, citrate ethanol, formate, D-galactose, H ₂ , carbonic acid, sodium, ammonium, Ni ²⁺ , nitric oxide, nitrite, nitrate, protoheme, urea

^a Min I, minimal medium; min II, minimal medium plus D-glucose; min III, minimal medium plus D-glucose plus alternative carbon sources; min IV, minimal medium plus D-glucose plus alternative carbon sources plus amino acids; rich medium, medium containing all compounds for which a transport system has been defined based on the work of Schilling et al. (39).

Medium composition. The composition of the in silico media used in this study was adapted from that described by Schilling et al. (39) (Table 1). In order to determine the minimal medium needed by *iIT341* GSM/GPR to fulfill the biomass requirement, each medium substrate was taken out of the rich medium containing all substrates for which corresponding transport systems had been defined. If the network was not capable of producing biomass without taking up a particular compound, that compound was deemed essential. The set of all essential compounds made up minimal medium I (Table 1). Minimal medium II contained D-glucose in addition to minimal medium I. Minimal medium III contained alternative carbon sources, which were also studied by Schilling et al. (39). Minimal medium IV contained all amino acids in addition to minimal medium III (Table 1). The uptake rates for protons and water were not constrained; the uptake rates of all other medium components were set to be maximally 20 mmol/h/g (dry weight). The oxygen uptake rate was set to be maximally 5 mmol/h/g (dry weight). These constraints were chosen arbitrarily, and they did not alter the observed growth phenotypes in single- and double-knockout deletions.

Deletion studies. In each single-gene-deletion experiment, we removed any reaction(s) associated with a particular gene from the network by constraining the corresponding reaction flux values to zero and then maximizing for growth. Gene deletion simulations that yielded a growth rate of less than 10^{-6} mmol/h/g (dry weight) in the tested medium were defined to be lethal. Each single-deletion experiment was performed with five different in silico media (Table 1). The reduction in growth rate upon deletion of a nonessential gene was determined by normalizing the growth rate of the mutant to that of the wild type in the same medium.

A double-deletion in silico experiment was performed by first identifying all reactions associated with two chosen genes and then setting the corresponding reaction fluxes to zero. Again, double-deletion mutants with growth rates less than 10^{-6} mmol/h/g (dry weight) in the tested medium were defined to be lethal. Double-deletion studies were carried out only in the rich medium, as the lethal double-knockout mutations found in this medium would also be lethal in the other media used in this study.

In this study, a gene was designated "essential" if its deletion resulted in a lethal mutation in all tested media. On the other hand, a "conditionally essential gene" was one whose deletion led to a lethal mutant in at least one medium but not in all. Last, we used the term "synthetic lethal genes" to describe pairs of

genes whose double deletion rendered biomass production impossible but neither of whose single deletion affects cell viability.

Deletion studies on essential reactions for each biomass component. We used the updated metabolic network to identify reactions that are necessary for the synthesis of each biomass constituent in *H. pylori*. This in silico experiment was carried out by sequentially removing every reaction from the network and then maximizing for the production of one biomass component at a time. A reaction was declared to be necessary with respect to a particular biomass component if the network was not able to produce that component in the absence of that reaction.

All calculations for this study were done using Matlab (Mathworks, Inc., Natick, MA), with Lindo (LINDO Systems Inc., Chicago, IL) as the linear-programming solver.

RESULTS

We present here an expanded genome-scale metabolic network of *H. pylori*, *iIT341* GSM/GPR, reconstructed based on the previously published network (39), the revised genome annotation (1), and up-to-date biochemical and physiological data. Novel features of *iIT341* GSM/GPR include (i) gene-protein-reaction associations, (ii) elementally and charge-balanced reactions, (iii) more accurate descriptions of isoprenoid and lipopolysaccharide metabolism, and (iv) quantitative assessments of the supporting data for each reaction. A detailed description of the network and a metabolic map containing all network reactions can be found in the supplemental data (see Table S2 and Figure S1 at <http://gcrp.ucsd.edu/organisms/hpylori.html>).

Properties of the *iIT341* GSM/GPR metabolic network. The updated reconstruction of *H. pylori*, *iIT341* GSM/GPR, accounts for 341 genes, 476 intracellular reactions, 78 exchange

TABLE 2. Comparison of *iCS291* and *iIT341* GSM/GPR

Parameter	<i>iCS291</i>	<i>iIT341</i> GSM/GPR	% Similarity
No. of genes included	291	341	83
No. of gene-associated reactions	272	354	68
No. of other reactions	116	113	61
No. of total reactions	388	476	66
No. of metabolites (internal/external)	339/64	411/74	70/80
No. of exchange fluxes ^a	115	74	
S matrix (no. of reactions × no. of metabolites) ^a	649 × 403	554 × 485	

^a Influxes and effluxes for each metabolite were written as separate unidirectional reactions in *iCS291* but were represented as reversible reactions in *iIT341* GSM/GPR.

reactions, and 485 metabolites. Thus, this network includes 50 new gene loci, 88 new reactions, and 82 more metabolites than does *iCS291* (Table 2). New gene loci were identified from careful searches of the literature and the PyloriGene database (created based on the revised genome annotation [1]). Most of the newly added reactions and metabolites resulted from introducing distinct steps for reactions that were lumped together in *iCS291*; examples are those in the lipopolysaccharide and isoprenoid pathways. After the existing data were reevaluated, five reactions present in *iCS291* were completely removed and not included in *iIT341* GSM/GPR. They included one enzymatic reaction (methionine synthase) and four transport reactions, for dipeptide, oligopeptide, polypeptide, and glycerol. The presence of the methionine synthase would enable the network to synthesize L-methionine, which was found to be an essential amino acid of *H. pylori* (34, 38). The transport reactions were removed because *iIT341* GSM/GPR does not account for peptide metabolism, due to incomplete information about further peptide conversions in *H. pylori*.

Each reaction in *iIT341* GSM/GPR was assigned a confidence level from 1 to 4 (see Table S2 in the supplemental data

at <http://gcrp.ucsd.edu/organisms/hpylori.html>) to reflect the strength of the supporting data. The criteria for assigning the confidence levels were designated as follows: 1, modeling purpose only; 2, sequence homology or physiological data; 3, genetic or proteomic data; and 4, direct biochemical data (47). The average confidence level of the reactions in *iIT341* GSM/GPR is approximately 2.5.

A biomass equation is often used to represent all compounds that are thought to be required for the growth of an organism (45). In this study, the *H. pylori* biomass equation accounted for 52 metabolites (see Table S3 in the supplemental data at <http://gcrp.ucsd.edu/organisms/hpylori.html>). The fractional contribution of each of these compounds was adapted from the biomass composition of *Escherichia coli* (35), with exceptions for phospholipids (cardiolipin, phosphatidylethanolamine, phosphatidylglycerol, and phosphatidylserine) for which *H. pylori*-specific data were available (15). Thiamine, biotin, protoheme, and menaquinone were also included in the biomass equation, even though their fractional contributions to the biomass have not been measured. These compounds were assumed to have a fractional contribution of 6×10^{-6} , which is equal to that of coenzyme A, the metabolite with one of the smallest fractional contributions in the biomass. Due to the nature of the linear-programming formulation, these assumed values may marginally affect the growth rate, but they usually do not change the result of a deletion experiment (46).

All metabolic pathways in the reconstruction were grouped into six different subsystems: central metabolism, amino acid metabolism, vitamin and cofactors, cell wall, nucleotide metabolism, and other (see Table S7 in the supplemental data at <http://gcrp.ucsd.edu/organisms/hpylori.html>). Analyses of gene distribution over subsystems showed that most genes can be found in the central metabolism subsystem (88 genes), followed by the vitamin and cofactor (62 genes) and the cell wall metabolism (60 genes) subsystems (Fig. 1A). The same scheme was employed to evaluate the distribution of reactions over subsystems (Fig. 1B). The vitamin and cofactor metabolism subsystem had the highest number of reactions (91 reactions).

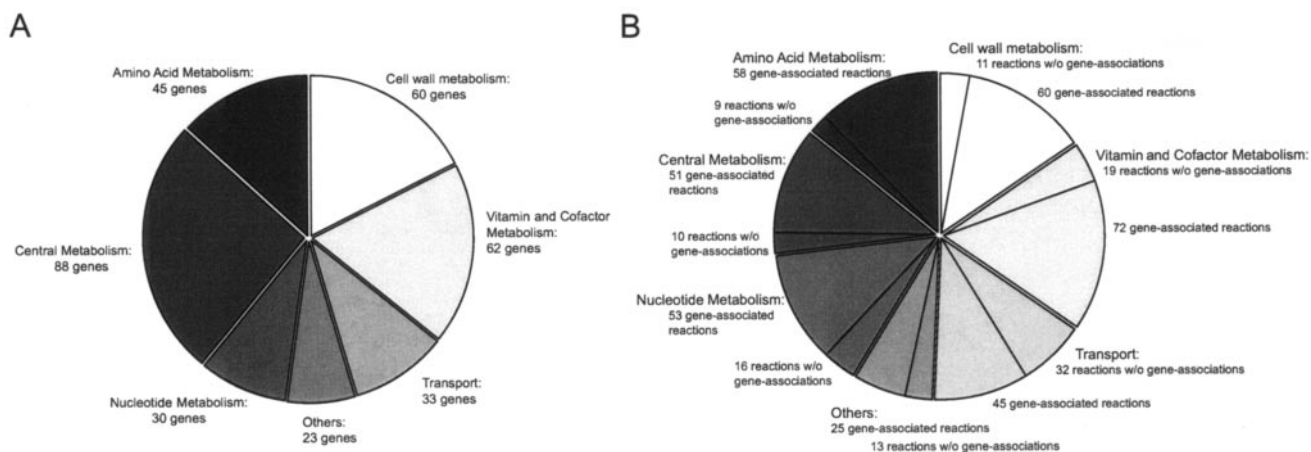


FIG. 1. Distributions of genes (A) and reactions (B) over subsystems. The reactions of each subsystem in panel B are additionally subcategorized into gene-associated and non-gene-associated reactions. w/o, without.

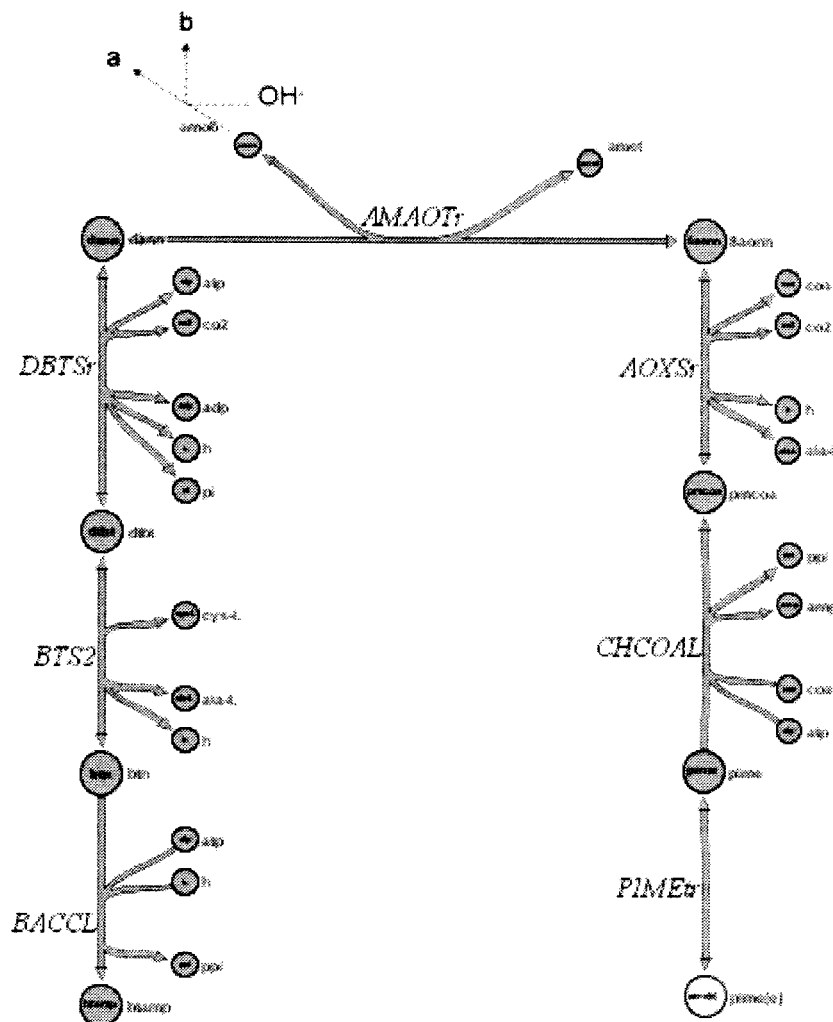


FIG. 2. Schematic representation of biotin biosynthesis. The dotted line represents the hypothetical downstream conversion of *S*-adenosyl-4-methylthio-2-oxobutanoate (amob) (43). Metabolites a and b represent 2-oxobut-3-enoate and 5'-methylthioadenosine, respectively. Reaction and metabolite abbreviations used here can be found in Table S2 in the supplemental data.

On the other hand, the central metabolism subsystem had the second-lowest number of reactions (61 reactions).

Identification and analysis of dead ends in *iIT341* GSM/GPR. Metabolites that are only consumed or only produced within the metabolic network are referred to as “dead ends” (37). Dead ends usually represent missing knowledge about the underlying biochemical pathways in an organism. Experimental analyses of these dead ends can help identify new reactions and pathways (37). Moreover, compounds that are experimentally verified to be dead ends are also useful in studying pathway evolution. In particular, they may suggest that either a complete pathway existed in some ancestral bacteria or that the associated gene was recently acquired but the entire pathway has not been completed. The complete version of *iIT341* GSM/GPR contains 48 dead-end metabolites (see Table S4 in the supplemental data at <http://gcrp.ucsd.edu/organisms/hpylori.html>). In the following paragraph, we describe the inconsistent data for one of these dead ends and our decision on how to resolve it. A more detailed discussion of other dead ends can

be found in the supplemental data (see section 1 at the above-cited website).

The synthesis of biotin is well studied in various organisms. Pimelate, a biotin precursor, is converted to biotin in five steps (Fig. 2). The third step is carried out by the adenosylmethionine-8-amino-7-oxononanoate transaminase (EC 2.6.1.62; abbreviated AMAOTr) (Fig. 2), which converts 8-amino-7-oxononanoate (8aonn) to 7,8-diaminononanoate (dann) and *S*-adenosyl-4-methylthio-2-oxobutanoate (amob). Stoner et al. suggested that amob may undergo a spontaneous reaction with hydroxide ions under alkaline conditions to form 5'-methylthioadenosine and 2-oxobut-3-enoate (43). However, even if this reaction takes place in the cell, the further use of 2-oxobut-3-enoate by the metabolic network is not clear. Therefore, in order for the biosynthesis of biotin to be used in the network, we created a reversible artificial reaction (sink_amob) to allow the network to consume and produce amob freely.

Minimal medium requirement of *iIT341* GSM/GPR. The minimal medium reported for *iCS291* contained 12 metabo-

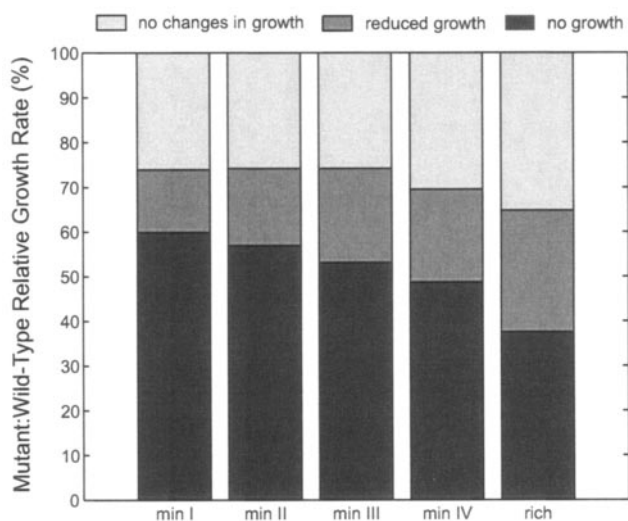


FIG. 3. Results of the in silico single-deletion studies. The growth rate percentages of lethal and nonlethal deletions are shown for each medium. The reduced-growth section indicates the percentage of mutants displaying reduced growth compared to that of the wild type in the same medium. See Table 1, footnote *a*, for medium abbreviations.

lites (39). We tested *iIT341* GSM/GPR to see whether the changes introduced in the updated model led to a different minimum set of required substrates. We found that, in contrast to *iCS291*, our model did not require cysteine or inorganic sulfate. Cysteine and methionine each contain a sulfur group that can be used by the network to synthesize sulfur-containing compounds such as biotin. Changes introduced in the methionine metabolism in *iIT341* GSM/GPR enabled it to utilize methionine as a sulfate source (see section 1 in the supplemental data at <http://gcr.g.ucsd.edu/organisms/hpylori.html> for details). In total, the minimal medium for *iIT341* GSM/GPR differed from that of *iCS291* by only three compounds: L-phenylalanine and sulfate (or L-cysteine) were required only in *iCS291*, and pimelate was required only in *iIT341* GSM/GPR, due to the changed biomass definition.

Single-deletion study: essential and conditionally essential genes. The presence of a large fraction of essential genes in a particular medium implies that *H. pylori* is especially adapted to its environment and has only limited ability to tolerate environmental disturbances (e.g., substrate supply, acidity, or mutagenic agents). In this study, we evaluated the fraction of genes that were essential in the five specified media. Our model predicted that a high percentage, 60%, of the total genes in the model were either essential or conditionally essential in minimal medium I. The percentage of genes found to be essential or conditionally essential decreased with increasing complexity of the medium and was lowest, 37.5%, in rich medium (Fig. 3). Notably, approximately 30% of the gene deletions were predicted to have no effect on the growth rate relative to that of the wild type in the same medium. In total, 128 genes out of 341 were predicted to be essential in all media tested. Another 75 conditionally lethal mutants were also identified in minimal medium I.

In classifying genes and reactions into subsystems, we were curious to see if a certain subsystem showed a larger number of essential genes than did others. As expected, most of the essential genes belong to two subsystems: cell wall (51 genes, 39%) and vitamin and cofactor (33 genes, 26%). The remaining 44 essential genes (45%) were distributed rather evenly among the other subsystems (Fig. 4A). Closer examinations of the distribution of conditionally essential mutations showed that a large number of conditionally essential mutations can be found in the amino acid (27%) and central metabolism (25%) subsystems, but only few in the cell wall subsystem (4%) (Fig. 4B).

Validation of predicted single-deletion growth phenotypes with experimental data. We used *iIT341* GSM/GPR to compute the essentiality of every gene in the network and compared the results with reported experimental data to assess the predictive capability of the model. Experimental data were available for 72 out of 341 mutants for comparison (Table 3). These experiments were usually carried out with rich media containing an agar base with either horse or sheep blood and

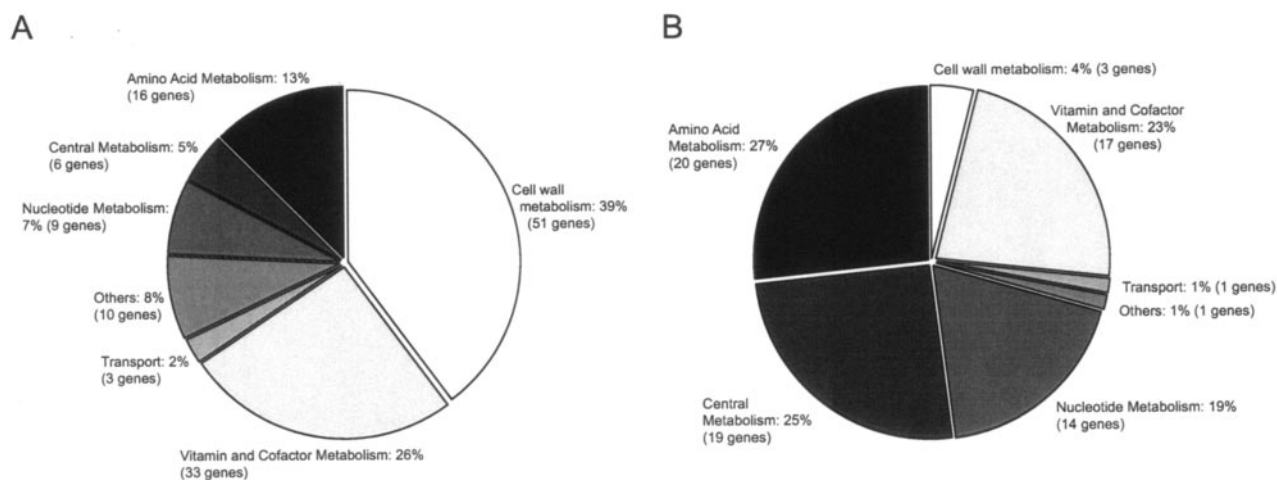


FIG. 4. Distributions of essential genes (A) and conditionally essential genes (B) over subsystems. The number of essential or conditionally essential genes per subsystem is shown in parentheses.

TABLE 3. Comparison of in silico predictions of single knockouts with experimental data

Gene locus	Gene name	Reaction name	Exptl data ^a						Reference	Medium compound that induces growth phenotype switch
			Min I	Min II	Min III	Min IV	Rich	Exp		
HP0002, HP1574	<i>ribD, ribG</i>	DB4PS	-	-	-	-	-	-	50	
HP0004, HP1186	<i>cynT, icfA</i>	H2CO3D	+	+	+	+	+	+	5	
HP0055	<i>putP</i>	PROt4r	+	+	+	+	+	+	18	
HP0067 to HP0070, HP0072 to HP0073	<i>ureH, ureG, ureF, ureE, ureB, ureA</i>	UREA	+	+	+	+	+	+	41	
HP0071	<i>ureI</i>	UREAt	+	+	+	+	+	+	18	
HP0075	<i>glmM, ureC</i>	PGAMT	-	-	-	-	-	-	7	
HP0086	<i>mgo</i>	MDH4	-	-	+	+	+	-	3	L-Asparagine, L-aspartate, L-threonine
HP0112	<i>fucA</i>	FCLPA	+	+	+	+	+	+	18	
HP0121	<i>ppsA</i>	PPS	-	+	+	+	+	+	18	D-Glucose
HP0191 to HP0193	<i>frdB, frdA, frdC</i>	FRD5	+	+	+	+	+	+	12, 18	
HP0197	<i>metK, metX</i>	METAT	-	-	-	-	-	-	18	
HP0212	<i>dapE</i>	SDPDS	-	-	-	-	-	-	21	
HP0215	<i>cdsA</i>	DASYN_HP	-	-	-	-	-	+	18	
HP0255	<i>purA</i>	ADSS	-	-	+	+	+	+	18	Adenine, adenosine
HP0293	<i>pabB</i>	PABB	-	-	-	-	-	+	18	
HP0329	<i>nadE</i>	NADS1	-	-	-	-	+	+	18	Nicotinamide D-ribonucleotide
HP0360	<i>galE</i>	UDPG4E	-	-	-	-	+	+	24	L-Galactose
HP0372	<i>dcd</i>	DCTPD, DCTPD2	+	+	+	+	+	+	3	
HP0380	<i>gdhA</i>	GLUDy	+	+	+	+	+	+	18	
HP0381	<i>hemG, hemK</i>	PPPGO	-	-	-	-	+	+	18	(Proto-) Heme
HP0389	<i>sodB, sodF</i>	SPODM	+	+	+	+	+	+	40	
HP0476	<i>gltX, gltX_1, gltX1</i>	GLUTRS	-	-	-	-	+	+	18	(Proto-) Heme
HP0509	<i>gldC</i>	GLYCTO1	-	-	-	-	-	-	3	
HP0512	<i>glnA</i>	GLNS	-	-	+	+	+	-	11	L-Glutamine
HP0588 to HP0591	<i>oorD, oorA, oorB, oorC</i>	OOR	-	-	-	-	-	-	3, 16	
HP0687	<i>feoB</i>	FE2abc	-	-	-	-	+	-	48	(Proto-) Heme
HP0735	<i>gpt</i>	GUAPRT, HXPRT, XPRT	+	+	+	+	+	-	3	
HP0740	<i>murF</i>	UGMDDS	-	-	-	-	-	-	3	
HP0802	<i>ribA</i>	GTPCII	-	-	-	-	-	-	10	
HP0804	<i>ribB</i>	DB4PS	-	-	-	-	-	-	10	
HP0808	<i>acpS</i>	ACPS	+	+	+	+	+	-	3	
HP0824-0825	<i>trx1, trxA, trxB, trxR1</i>	TRDR	-	-	-	-	-	-	3	
HP0829	<i>guaB</i>	IMPd	-	-	+	+	+	+	18	Guanine, xanthine
HP0832	<i>speE</i>	SPMS	-	-	-	-	-	+	3	
HP0875	<i>kata</i>	CAT	+	+	+	+	+	+	13, 18	
HP1011	<i>pyrD</i>	DHORD3	-	-	-	-	+	-	6	Orotate, uracil
HP1038	<i>aroD, aroQ</i>	DHQD	-	-	-	-	-	-	3	
HP1050	<i>thrB</i>	HSK	-	-	-	+	+	+	18	L-Threonine
HP1052	<i>envA, lpxC</i>	UHGADA_HP	-	-	-	-	-	+	18	
HP1077	<i>nixA</i>	NIabc	+	+	+	+	+	+	18	
HP1084	<i>pyrB</i>	ASPCT	-	-	-	-	+	-	2	Orotate, uracil
HP1087	<i>ribC</i>	RBFSa, RBFSb	-	-	-	-	-	-	10	
HP1091	<i>kgtP</i>	AKGt2r	+	+	+	+	+	+	18	
HP1099	<i>eda</i>	EDA	+	+	+	+	+	-	3	
HP1100	<i>edd</i>	EDD	+	+	+	+	+	-	3	
HP1100	<i>edd</i>	EDD	+	+	+	+	+	+	49	
HP1108 to HP1111	<i>porG, porD, porA, porB</i>	PDH2	-	-	-	-	+	-	3	Thymidine + acetate
HP1108 to HP1111	<i>porG, porD, porA, porB</i>	PDH2	-	-	-	-	+	+	17	Thymidine + acetate
HP1118	<i>ggt</i>	GTMLT	+	+	+	+	+	+	4, 18	
HP1180	<i>nupC</i>	ADNt2, ADNt2, CYTDt2, DADNt2, DCYTt2, DURIt2, THMDt2, URIt2	+	+	+	+	+	+	18	
HP1257	<i>pyrE</i>	ORPT	-	-	-	-	+	-	3	Uracil
HP1385	<i>fbp</i>	FBP	-	+	+	+	+	-	3	D-Glucose
HP1399	<i>rocF</i>	ARGN	-	-	-	+	+	+	26	Ornithine, L-proline
HP1418	<i>murB</i>	UAPGR	-	-	-	-	-	-	3	
HP1491		Pit2r	-	-	-	-	-	+	18	
HP1495	<i>tal</i>	TALA	+	+	+	+	+	+	3	
HP1505	<i>ribD</i>	APRAUR, DHPPDA	-	-	-	-	-	-	10	

^a Boldface indicates results of experiments that agreed with in silico predictions. Exp, in vivo study results. +, growth under the given condition; -, lethal deletion. See Table 1, footnote a, for medium abbreviations. Reaction abbreviations used here can be found in Table S2 in the supplemental data.

antibiotics, but the detailed chemical compositions of the media were not reported (Becton, Dickinson and Company, Franklin Lakes, NJ). We therefore felt that it was most appropriate to compare these data with our results with minimal

medium IV and with rich medium (Table 3). The model correctly predicted 73% and 75% of gene deletion experiments for the 72 mutants when compared to the results with minimal medium IV and rich medium, respectively.

Predictive capability of *iIT341* GSM/GPR compared to that of previous reconstruction *iCS291*. To verify that *iIT341* GSM/GPR represents a more accurate description of *H. pylori* metabolism than does *iCS291*, we quantitatively evaluated its improvement on gene essentiality prediction. We first identified common genes in both reconstructions for which experimental gene essentiality data were available (Table 3). Then, we applied the same medium conditions to both models to calculate the effect of these genes on growth rates. In total, *iIT341* GSM/GPR predicted 44 out of 59 (75%) deletion experiments correctly, while *iCS291* was correct only in 41 out of 59 cases (69%); both results were with minimal medium IV. In rich medium *iIT341* GSM/GPR predicted 42 phenotypes (71%) correctly, while *iCS291* achieved only 37 (63%) correct predictions. Taken together, these results show that *iIT341* GSM/GPR is more accurate at predicting gene essentiality.

Analysis of false predictions. The analysis of false predictions by the models is also informative and can be used to either update the model or reevaluate experimental data. For example, both models failed to predict the essentiality of HP1100 (6-phosphogluconate dehydratase [EDD]) and HP1099 (2-dehydro-3-deoxy-phosphogluconate aldolase [EDA]), which have been found essential by Chalker et al. (3). However, Wanken et al. were able to grow HP1100 mutants (49). The gene products of HP1100 and HP1109 are part of the Entner-Doudoroff pathway, which *H. pylori* can use as an alternative to the glycolytic pathway to metabolize D-glucose (25, 30). Other experimental observations (25, 31) also showed that *H. pylori* is not dependent on D-glucose as a carbon source. Our model predictions were found to be consistent with the last three studies mentioned.

In addition, our model did not predict HP0832 to be essential. Chalker et al. suggested that HP0020 (carboxynorspermidine decarboxylase) could replace HP0832 in catalyzing the last step of the spermidine biosynthesis pathway in *H. pylori* (3). However, HP0020 was not included in the reconstruction, since its function as spermidine synthetase (SPMS) was not confirmed experimentally. Last, in contrast to *iCS291*, our model did not correctly predict the essentiality of HP0808 (acyl carrier protein synthase [ACPS]). The reason for this is that two steps of the pantothenate biosynthesis were lumped together in *iIT341* GSM/GPR (EC 2.7.87 and 3.1.4.14) to avoid including an apoprotein. As a consequence, this reaction does not account for the acyl carrier protein, rendering the gene nonessential in silico.

For certain knockout mutants, the in silico predictions were false for only a subset of tested media. In order to determine which compounds in the media rendered these phenotype switches, we carried out a more detailed analysis. Each compound was added separately to minimal medium I, and then the deletion experiments in silico were repeated. For example, HP0086 (malate dehydrogenase; EC 1.1.99.16) was essential only when L-aspartate, L-asparagine, or L-threonine was not available in the in silico medium (Table 3, last column). Interestingly, we found that the mutant with deleted pyruvate dehydrogenase (PDH2; encoded by HP1108 to HP1111) was viable when both thymidine and acetate were added to the medium. Therefore, differences in medium conditions might explain the conflicting experimental results by Chalker et al. (3) and Hughes et al. (16) for the pyruvate dehydrogenase

mutants. The complete list of results of this deletion study can be found in Tables S5 and S6 of the supplemental data at <http://cgcr.ucsds.edu/organisms/hpylori.html>.

Nonlethal single-knockout mutants with reduced growth rates. The reduction in growth rates of the mutants relative to that of the wild type in the same medium reflects the importance of the deleted genes within the metabolic network (Fig. 5). The knockout of genes involved in the respiratory chain (genes for BC10, CYOO_HP, and ATPS4r) was not strictly essential but led to reduced growth rates of the mutants relative to that of the wild type in the same medium (Fig. 5). This observation indicated that the network was mainly using the respiratory chain for ATP production under substrate-limiting conditions, while the presence of other carbon sources enabled it to produce energy via pathways other than oxidative phosphorylation. We found that the amount of reduction in the growth rate decreased with the increasing complexity of the medium. Reduced growth of the mutant relative to the wild type in the same medium also allowed for the evaluation of substrate usage. For example, the deletion of HP1100 or HP1103, whose gene products (EDD and HEX1) are necessary to metabolize D-glucose, led to a 60% decrease in growth rate relative to that of the wild type in minimal medium II (which contained D-glucose in addition to minimal medium I). The addition of alternate carbon sources (as in minimal medium III) restored 90% of the growth rate observed in the wild type. This result indicated that the mutant, as well as the wild type, can metabolize alternate carbon sources efficiently. In fact, experimental studies found that *H. pylori* uses D-glucose only when most other energy sources have been depleted (31).

Double-deletion mutants of *iIT341* GSM/GPR. Double-deletion experiments are generally difficult to perform on a large scale in vivo. In silico models provide tools to rapidly predict the phenotype of such double-knockout mutants in various media. Here we carried out double-deletion studies in rich medium for every pair of genes identified as nonessential in single-deletion studies (Table 4). In total, more than 22,000 possible double-knockout mutants were screened. We identified 47 conditionally lethal double mutants, involving 64 different metabolic genes, for *iIT341* GSM/GPR. These synthetic essential genes represented almost 18% of all genes included in the model and 30% of all nonessential genes in rich medium. Most lethal synthetic mutants were found when a gene of a particular pathway and a gene for the transport for either the precursor or product of this pathway were deleted. For example, deletion of urease (HP0067 to HP0070, HP0072, and HP0073) and the urea transporter (HP0071) together led to a lethal synthetic mutant (Table 4). This result was interesting because neither did *H. pylori* require urea in media nor was urease (UREA, HP0067 to HP0070, HP0072, and HP0073) found essential in rich medium (Table 3).

Required reactions for the production of each biomass compound. We carried out reaction deletion studies to determine which network reactions are necessary for the production of each biomass constituent. Here, we simulated reaction deletions instead of gene deletions, so that we could also consider non-gene-associated reactions in the network. We removed one reaction at a time from the network and then maximized the production of each biomass compound. Biomass compounds were grouped based on the reactions needed for their

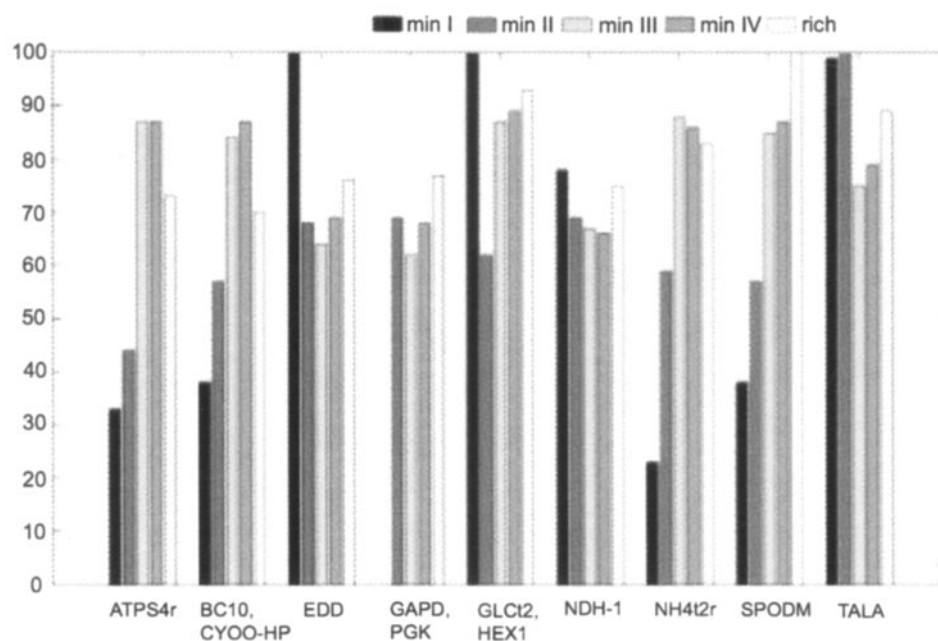


FIG. 5. Variation in growth rate observed in single knockouts of nonessential genes. The percentage growth rate was calculated relative to that of the wild type under the same medium conditions. The reaction abbreviations used here can be found in Table S2 of the supplemental data at <http://gcrucg.ucsd.edu/organisms/hpylori.html>. See Table 1, footnote *a*, for medium abbreviations.

syntheses. The first cluster accounted for 46 out of 52 biomass compounds. The syntheses of compounds in this cluster required 90 reactions on average, with a minimum of 80 reactions (Table 5). The second cluster included mostly phospholipids. Their synthesis required a common set of 17 metabolic reactions, with an average of 19 reactions. There were two biomass compounds, 5-methyltetrahydrofolate (5mthf) and lipopolysaccharide (lps_hp), that did not have the same set of required reactions as the other two groups of biomass compounds. The syntheses of 5mthf and lps_hp required 34 and 45 reactions, respectively; these two sets of reactions did not overlap. It is notable that only two biomass compounds, spermidine (sprm) and 5mthf, required oxygen uptake (O2tr) for their production.

In some cases, only one reaction in a pathway was required for the synthesis of a particular biomass constituent (Table 5), as was the case for malate synthase (MALS) (tricarboxylic acid cycle) in the synthesis of 5mthf. This suggests that such reactions are also involved in pathways other than those with which they have been traditionally associated. In many other cases, however, all reactions in the entire pathway were needed for the synthesis of a biomass constituent. Examples are reactions in the menaquinone biosynthesis and methionine salvage pathways (Table 5).

DISCUSSION

In this study, we presented an updated reconstruction of the metabolism of the human pathogen *H. pylori* based on the revised genome annotation (1) and new experimental data. This reconstruction represents a detailed review of the current knowledge about *H. pylori*, integrating biochemical and genomic data in a comprehensive framework including gene-

protein-reaction associations. The reconstruction was used to perform genome-scale single- and double-deletion studies and to determine required reactions for the synthesis of each biomass compound.

H. pylori is a fastidious organism with a small genome. The small number of predicted open reading frames (approximately 1,600) (1) reflects its adaptation to its natural niche of the human stomach, where the pathogen does not encounter much competition from other microorganisms (33). Results of our single- and double-deletion studies support this notion, as the high number of essential genes indicates a low redundancy in the metabolic network. More than half of the included metabolic genes were found to be required in tested minimal medium, suggesting a weak ability of the metabolic network to accommodate changes in acidity, nutrients, and temperature in the environment.

Gene deletion experiments yield information about the function of the deleted genes with respect to the overall metabolism of an organism. The model failed to correctly predict growth phenotypes of a subset of single-knockout deletions (Table 3). Various reasons could explain these false predictions. For example, the genome of *H. pylori* has a large number of hypothetical annotated open reading frames that may encode enzymes that either catalyze some of the non-gene-associated reactions or perform undiscovered functions in *H. pylori*. Therefore, it is possible that not all metabolic capabilities of *H. pylori* were included in *iIT341* GSM/GPR. False-negative predictions often reflect such incomplete or missing pathways. *iIT341* GSM/GPR predicted five false-negative growth phenotypes, which were associated with five different pathways (in minimal medium IV and rich medium) (Table 3). In contrast, false-positive predictions often suggest missing knowledge in

TABLE 4. Conditionally lethal mutants^a

Gene locus I (reaction)	Gene locus II (reaction)
HP0067 to HP0070, HP0072 to HP0073 (UREA)	HP0071 (UREAt)
HP0121 (PPS)	HP1102 (PGL); HP0154 (ENO); HP0974 (PGM); HP1345 (PGK); HP1346, HP0921 (GAPD)
HP0572 (ADPT)	HP0255 (ADSS), HP1112 (ADSL1r, ADSL2r)
HP0577 (FTHFLi, MTHFC, MTHFD)	HP0183 (GHMT2r)
HP0646 (GALU)	HP0360 (UDPG4E), HP1174 (GALt2, GLCt2)
HP0724 (ASNt2, ASPt2r, MALt2r, SUCCt2, SUCFUMti)	HP0191-93 (FRD5)
HP0735 (GUAPRT, HXPRT, XPPT)	HP0409 (GMPS2)
HP1169 to HP1172 (GLNabc)	HP0512 (GLNS)
HP1174 (GALt2, GLCt2)	HP0360 (UDPG4E), HP0646 (GALU)
HP1179 (PPM, PPM2)	HP0574 (RPI)
HP1180 (ADNt2, CYTDt2, DADNt2, DCYTt2, DURIt2, THMDt2, URIIt2)	HP1108 to HP1111 (PDH2), HP1533 (TMDSf)
HP1189 (ASAD)	HP0106 (METB1r), HSERTA
HP1227, HP1538 to HP1540 (BC10)	HP0875 (CAT)
HP1290 (NMNTP)	HP0329 (NADS1), HP1355 (NNDPR), HP1356 (QULNS), ASPO2
HP1337 (NMNAT, NNAT)	HP0329 (NADS1), HP1355 (NNDPR), HP1356 (QULNS), ASPO2
HP1461 (CCP)	HP0875 (CAT)
HP1495 (TALA)	HP0574 (RPI), HP1386 (RPE)
ADD	HP0572 (ADPT)
CYSabc	HP0107 (CYSS), HP1210 (SERAT)
FUMt3	HP1325 (FUM)
GALK	HP0360 (UDPG4E), HP0646 (GALU)
GALTi	HP0360 (UDPG4E), HP0646 (GALU)
HEMEti	HP0163 (PPBNGS), HP0237 (HMBS); HP0239 (GLUTRR); HP0306 (G1SATi); HP0376 (FCLT); HP0381 (PPPGO); HP0476, HP0643 (GLUTRS); HP0604 (UPPDC1, UPPDC2); HP0687 (FE2abc); HP1224 (UPP3S); HP0665, HP1226 (CPPPGO)
LYSt2r	HP0290 (DAPDC)
PGMT	HP0360 (UDPG4E), HP1174 (GALt2, GLCt2), GALK, GALTi
PHEt2r	HP0291 (CHORM), HP0672 (EHGLAT, PHETA1, TYRTA), PPNDH
THRt2r	HP0098 (THRS), HP1189 (ASAD), HP1050 (HSK)
TRPt2r	HP1279 (IGPS, PRAi), HP1280 (ANPRT)
TYRt2r	HP0291 (CHORM), HP1380 (PPND)
UPPRT	HP0005 (OMPDC), HP1257 (ORPT)
URAt2	HP0005 (OMPDC), HP1257 (ORPT)

^a A double deletion of a gene in the first column and a gene in the second column is predicted to result in a lethal phenotype. All of the genes listed here are nonessential in single-deletion studies. Reaction abbreviations used here can be found in supplemental material Table S2.

TABLE 5. Required reactions for the synthesis of biomass constituents in rich medium^a

Pathway ^b	Reaction abbreviation(s)	Synthesis of biomass constituent ^c																							
		accoa(c)	MI	bin(c)	ctp(c), dep(c)	dgtp(c), gtp(c)	fad(c)	mqrn6(c)	nadh(c), nadhph(c)	spmd(c)	succoa(c)	udpg(c), utp(c)	M2	ala-L(c)	coa(c)	dttp(c)	met-L(c)	nadh(c)	peptido-EC(c)	5mthf(c)	clpn-HP(c)	pc-HP(c)	pg-HP(c)	ps-HP(c)	lps-HP(c)
Amino acid degradation	VALTA	X								X			X												
Amino sugar metabolism	UAGDP2, GF6PTA, PGAMT, G1PACT, UAGDP, UAGCVT, UAPGR	X	X	X	X	X	X	X	X	X	X	X	X	X	X	X	X	X	X	X					X
ATP de novo synthesis	ADK1	X	X	X	X	X	X	X	X	X	X	X								X	X	X	X	X	
Biotin biosynthesis	CHCOAL, AOXSr, AMAOTr, DBTSr, BTS2	X	X	X	X	X	X	X	X	X	X	X		X	X	X	X	X	X	X					
Chorismate biosynthesis	DDPA, DHQS, DHQD, SHK3Dr, SHKK, PSCVT, CHORS						X												X						
dNTP biosynthesis	RNDR1, NDPK8, RNDR3, NDPK7, RNDR2, NDPK5, NDPK4	X	X	X	X	X	X	X	X	X	X	X	X	X	X	X	X	X	X	X					
Fatty acid synthesis	ACCOACr, MCOATA, C140SN, C160SN, C180SN, C181SN, C190cSN, KAS-HP, KAS-HP2	X	X	X	X	X	X	X	X	X	X	X	X	X	X	X	X	X	X	X	X	X	X	X	X
Folate biosynthesis	DHFRi, GTPCI, DNTPPA, DNMPPA, DHNPA, ADCL, PABB, DHFS																		X						
Fucose biosynthesis	MAN6PI, PMANM, MAN1PT2r, GMAND, GFUCS	X	X	X	X	X	X	X	X	X	X	X	X	X	X	X	X	X	X	X					X
Glycerolipid synthesis	CLPNS-HP, GLYK, DASYN-HP, PSSA-HP, PGSA-HP, PGPP-HP, PSD-HP, PSSA-HP																			X	X	X	X		
Glycolysis	TPI																			X	X	X	X		
GTP de novo synthesis	GK1, NDPK1	X	X	X	X	X	X	X	X	X	X	X	X	X	X	X	X	X	X	X	X	X	X		
IMP synthesis	PRPPS	X	X	X	X	X	X	X	X	X	X	X		X			X		X	X	X	X	X		
Isoprenoid biosynthesis	DXPS, DXPRIi, MEPCT, CDPMEK, MECDPS, MECOPDH, DMPPS, IPDPS						X																		
LPS biosynthesis	S7PI, GMHEPK, GMHEPPA, GMHEPAT, AGMHE, RFA-HP, A5PISO, KDOPS, KDOPP, KDOCT, UAGAAT-HP, UHGADA-HP, U23GAAT-HP, USHD-HP, U2GAAT, U2GAAT2, LPADSS-HP, MOAT-HP, RFAC-HP, LPSSYN-HP	X	X	X	X	X	X	X	X	X	X	X	X	X	X	X	X	X	X	X					X
Lysine/threonine biosynthesis	DHDPS, DHDPry, THDPS, SDPTA, SDPDS, DAPE	X	X	X	X	X	X	X	X	X	X	X	X	X	X	X	X	X	X	X					
Menaquinone biosynthesis	ICHORSi, OXGDC2, SHCHCS2, SUCBZS, SUCBZL, NPHS, DHNAOT2, AMMQT6						X																		
Methionine salvage pathway	DKMPPD, MDRPDr, MTAN, MTRI, MTRK, UNK2	X	X	X	X	X	X	X	X	X	X	X	X	X	X	X	X	X	X	X					

Continued on following page

Downloaded from <http://jlb.asm.org/> on February 28, 2021 by guest

TABLE 5—Continued

Pathway ^b	Reaction abbreviation(s)	Synthesis of biomass constituent ^c																							
		accoa(c)	M1	bin(c)	ctp(c), dctp(c)	dgtp(c), gtp(c)	fad(c)	mqm6(c)	nadp(c), nadph(c)	spmd(c)	succoa(c)	udpg(c), utp(c)	M2	ala-L(c)	coa(c)	dtrp(c)	met-L(c)	nadh(c)	peptido-EC(c)	5mtf(c)	clpn-HP(c)	pc-HP(c)	pg-HP(c)	ps-HP(c)	lps-HP(c)
Nucleotide Interconversion	CYTK1, NDPK3	X					X		X				X								X	X	X	X	X
	DTMPK	X	X	X	X	X	X	X	X	X	X	X	X	X	X	X	X	X	X	X					
Nicotinate biosynthesis	NADK							X																	
	GCALDDr, GLYCTO1																			X					
Others	GLUR	X	X	X	X	X	X	X	X	X	X	X	X	X	X	X	X	X	X	X					
	PPA	X	X	X	X	X	X	X	X	X	X	X		X				X	X	X	X	X	X	X	X
Pantothenate/CoA biosynthesis	MOHMT, DPR, ASP1DC, PANTS, PNTK, PPNCL2, PPCDC, PTPATi, DPCOAK	X								X				X											
	UAMAS, UAMAGS, UAAGDS, ALAALAr, UGMDDS, PAPPT3, UAGPT3, PPTGS, UDPCDP	X	X	X	X	X	X	X	X	X	X	X	X	X	X	X	X	X	X	X					
Respiratory chain	FRDO	X	X	X	X	X	X	X	X	X	X	X	X	X	X	X	X	X	X	X					
Riboflavin metabolism	GTPCII, DHPPDA, APRAUR, PMDPHT, D84PS, RBFSa, RBFSb, RBFK, FMNAT						X																		
Spermidine biosynthesis	ARGDC, AGMT, ADMDCr, SPMS	X	X	X	X	X	X	X	X	X	X	X	X	X	X	X	X	X	X	X					
	METAT			X			X	X													X	X	X	X	X
TCA cycle	OOR	X	X	X	X	X	X	X	X	X	X	X	X	X	X	X	X	X	X	X					
	MALS																				X				
THF metabolism	MTHFR2																				X				
Thioredoxin system	TRDR	X	X	X	X	X	X	X	X	X	X	X	X	X	X	X	X	X	X	X					
	O21																								X
Transport	PIMEtr	X	X	X	X	X	X	X	X	X	X	X		X	X	X	X	X	X	X					X
	PII2r	X	X		X	X		X	X	X				X	X		X					X	X	X	X
	HISabc, ILEabc, LEUabc, THMabc, VALabc	X	X	X	X	X	X	X	X	X	X	X	X	X	X	X	X	X	X	X					
	METabc			X			X										X				X	X	X	X	
Tyr, Phe, Trp biosynthesis	CHORM																								
UTP/CTP de novo synthesis	UMPk	X	X	X	X	X	X	X	X	X	X	X	X	X	X	X	X	X	X	X					X
	NDPK2				X						X									X					X
	CTPS1				X																				
Others	DMATT, GRIT, OCTDPS						X																		
	sink-ahcys(c)						X														X	X	X	X	
	sink-amob	X	X	X	X	X	X	X	X	X	X	X	X	X	X	X	X	X	X	X	X	X	X	X	

^a Reaction and metabolite abbreviations used here can be found in Table S2 in the supplemental material.

^b dNTP, deoxynucleoside triphosphate; TCA, tricarboxylic acid.

^c X, lethal deletion; blank cell, viable deletion. M1 and M2 columns represent the two largest clusters. M1: amp(c), atp(c), datp(c), and nad(c). M2: thm(c), thr-L(c), trp-L(c), tyr-L(c), arg-L(c), asn-L(c), asp-L(c), val-L(c), cys-L(c), gln-L(c), h2o(c), his-L(c), ile-L(c), leu-L(c), lys-L(c), phe-L(c), peme(c), pro-L(c), ptrc(c), ser-L(c), glu-L(c), and gly(c). The symbol (c) signifies a cytosolic localization of the metabolite.

the biomass function. In our comparison, six single-deletion growth phenotypes were false positive, which were again associated with six different pathways. In addition, results for conditionally essential mutations were strongly dependent on the

composition of the tested medium (Table 3). The compositions of media used in in vivo experiments are usually not well documented in the literature. Without this knowledge, it is difficult to analyze the false predictions made by the network,

as the source of the discrepancy can lie in either the compositions of the media or the contents of the network.

The knowledge about in silico-predicted double-knockout mutants can help to reduce time and costs in designing in vivo experiments, and no such study is currently found in the literature for *H. pylori*. A genome-scale screening for such double-knockout mutants would be extremely difficult, since 213 out of 341 metabolic genes included in the model were not essential in at least one of the tested media. Thus, more than 22,000 double mutants would have to be tested in vivo to identify all lethal double-knockout mutants. These numbers highlight the value of in silico modeling for experimental design.

In this study, we provided an example of how a mathematical and systemic approach to data integration can be useful in predicting results for genome-scale experiments and in assessing properties of a metabolic network as a whole. This study also highlighted gaps in *H. pylori* metabolism where our knowledge is incomplete. We envision that additional studies on less-characterized pathways, such as those in norspermidine or molybdate metabolism, or the inclusion of regulatory elements in the computational models will greatly improve the model's predictive capability in the future and expand knowledge about *H. pylori* metabolism.

ACKNOWLEDGMENTS

We acknowledge Jennifer Reed, Andrew Joyce, Scott Becker, and Jason Papin for help and advice with the reconstruction process.

Funding for this work was provided by the Thieles and the San Diego Fellowship to T.D.V.

B.Ø.P. serves on the Scientific Advisory Board of Genomatica, Inc.

REFERENCES

- Boneca, I. G., H. de Reuse, J. C. Epinat, M. Pupin, A. Labigne, and I. Moszer. 2003. A revised annotation and comparative analysis of *Helicobacter pylori* genomes. *Nucleic Acids Res.* **31**:1704–1714.
- Burns, B. P., S. L. Hazell, G. L. Mendz, T. Kolesnikow, D. Tillet, and B. A. Neilan. 2000. The *Helicobacter pylori* pyrB gene encoding aspartate carbamoyltransferase is essential for bacterial survival. *Arch. Biochem. Biophys.* **380**:78–84.
- Chalker, A. F., H. W. Minehart, N. J. Hughes, K. K. Koretke, M. A. Lonetto, K. K. Brinkman, P. V. Warren, A. Lupas, M. J. Stanhope, J. R. Brown, and P. S. Hoffman. 2001. Systematic identification of selective essential genes in *Helicobacter pylori* by genome prioritization and allelic replacement mutagenesis. *J. Bacteriol.* **183**:1259–1268.
- Chevalier, C., J. M. Thiberge, R. L. Ferrero, and A. Labigne. 1999. Essential role of *Helicobacter pylori* gamma-glutamyltranspeptidase for the colonization of the gastric mucosa of mice. *Mol. Microbiol.* **31**:1359–1372.
- Chirica, L. C., C. Petersson, M. Hurlig, B. H. Jonsson, T. Boren, and S. Lindskog. 2002. Expression and localization of alpha- and beta-carbonic anhydrase in *Helicobacter pylori*. *Biochim. Biophys. Acta* **1601**:192–199.
- Copeland, R. A., J. Marcinkeviciene, T. S. Haque, L. M. Kopcho, W. Jiang, K. Wang, L. D. Ecret, C. Sizemore, K. A. Amsler, L. Foster, S. Tadesse, A. P. Combs, A. M. Stern, G. L. Trainor, A. Slee, M. J. Rogers, and F. Hobbs. 2000. *Helicobacter pylori*-selective antibacterials based on inhibition of pyrimidine biosynthesis. *J. Biol. Chem.* **275**:33373–33378.
- De Reuse, H., A. Labigne, and D. Mengin-Lecreulx. 1997. The *Helicobacter pylori* ureC gene codes for a phosphoglucosamine mutase. *J. Bacteriol.* **179**:3488–3493.
- Duarte, N. C., M. J. Herrgard, and B. Palsson. 2004. Reconstruction and validation of *Saccharomyces cerevisiae* iND750, a fully compartmentalized genome-scale metabolic model. *Genome Res.* **14**:1298–1309.
- Edwards, J. S., R. Ramakrishna, C. H. Schilling, and B. O. Palsson. 1999. Metabolic flux balance analysis, p. 13–57. *In* S. Y. Lee and E. T. Papoutsakis (ed.), *Metabolic engineering*. Marcel Dekker, Inc., New York, N.Y.
- Fassbinder, F., M. Kist, and S. Bereswill. 2000. Structural and functional analysis of the riboflavin synthesis genes encoding GTP cyclohydrolase II (ribA), DHBP synthase (ribBA), riboflavin synthase (ribC), and riboflavin deaminase/reductase (ribD) from *Helicobacter pylori* strain P1. *FEMS Microbiol. Lett.* **191**:191–197.
- Garner, R. M., J. Fulkerson, Jr., and H. L. T. Mobley. 1998. *Helicobacter pylori* glutamine synthetase lacks features associated with transcriptional and posttranslational regulation. *Infect. Immun.* **66**:1839–1847.
- Ge, Z., Q. Jiang, M. S. Kalisiak, and D. E. Taylor. 1997. Cloning and functional characterization of *Helicobacter pylori* fumarate reductase operon comprising three structural genes coding for subunits C, A and B. *Gene* **204**:227–234.
- Harris, A. G., F. E. Hinds, A. G. Beckhouse, T. Kolesnikow, and S. L. Hazell. 2002. Resistance to hydrogen peroxide in *Helicobacter pylori*: role of catalase (KatA) and Fur, and functional analysis of a novel gene product designated 'KatA-associated protein', KapA (HP0874). *Microbiology* **148**:3813–3825.
- Hazell, S. L., and G. L. Mendz. 1997. How *Helicobacter pylori* works: an overview of the metabolism of *Helicobacter pylori*. *Helicobacter* **2**:1–12.
- Hirai, Y., M. Haque, T. Yoshida, K. Yokota, T. Yasuda, and K. Oguma. 1995. Unique cholesteryl glucosides in *Helicobacter pylori*: composition and structural analysis. *J. Bacteriol.* **177**:5327–5333.
- Hughes, N. J., C. L. Clayton, P. A. Chalk, and D. J. Kelly. 1998. *Helicobacter pylori* porC/DAB and oorDABC genes encode distinct pyruvate:flavodoxin and 2-oxoglutarate:acceptor oxidoreductases which mediate electron transport to NADP. *J. Bacteriol.* **180**:1119–1128.
- Hughes, N. J., D. J. Kelly, A. A. Davison, P. A. Chalk, and C. L. Clayton. 1995. Characterisation of *Helicobacter pylori* pyruvate:flavodoxin oxidoreductase. *Gut* **37**:A18.
- Jenks, P. J., C. Chevalier, C. Ecobichon, and A. Labigne. 2001. Identification of nonessential *Helicobacter pylori* genes using random mutagenesis and loop amplification. *Res. Microbiol.* **152**:725–734.
- Kanehisa, M. 1997. A database for post-genome analysis. *Trends Genet.* **13**:375–376.
- Kanehisa, M., and S. Goto. 2000. KEGG: Kyoto encyclopedia of genes and genomes. *Nucleic Acids Res.* **28**:27–30.
- Karita, M., M. L. Etterbeek, M. H. Forsyth, M. K. R. Tummuru, and M. J. Blaser. 1997. Characterization of *Helicobacter pylori* dapE and construction of a conditionally lethal dapE mutant. *Infect. Immun.* **65**:4158–4164.
- Kauffman, K. J., P. Prakash, and J. S. Edwards. 2003. Advances in flux balance analysis. *Curr. Opin. Biotechnol.* **14**:491–496.
- Kelly, D. J. 1998. The physiology and metabolism of the human gastric pathogen *Helicobacter pylori*. *Adv. Microb. Physiol.* **40**:137–189.
- Kwon, D. H., J. S. Woo, C. L. Perng, M. F. Go, D. Y. Graham, and F. A. El-Zaatari. 1998. The effect of galE gene inactivation on lipopolysaccharide profile of *Helicobacter pylori*. *Curr. Microbiol.* **37**:144–148.
- Marais, A., G. L. Mendz, S. L. Hazell, and F. Mégraud. 1999. Metabolism and genetics of *Helicobacter pylori*: the genome era. *Microbiol. Mol. Biol. Rev.* **63**:642–674.
- McGee, D. J., F. J. Radcliff, G. L. Mendz, R. L. Ferrero, and H. L. T. Mobley. 1999. *Helicobacter pylori* rocF is required for arginase activity and acid protection in vitro but is not essential for colonization of mice or for urease activity. *J. Bacteriol.* **181**:7314–7322.
- Menz, G. L., B. P. Burns, and S. L. Hazell. 1995. Characterisation of glucose transport in *Helicobacter pylori*. *Biochim. Biophys. Acta* **1244**:269–276.
- Menz, G. L., and S. L. Hazell. 1995. Amino acid utilization by *Helicobacter pylori*. *Int. J. Biochem. Cell Biol.* **27**:1085–1093.
- Menz, G. L., and S. L. Hazell. 1991. Evidence for a pentose phosphate pathway in *Helicobacter pylori*. *FEMS Microbiol. Lett.* **84**:331–336.
- Menz, G. L., S. L. Hazell, and B. P. Burns. 1994. The Entner-Doudoroff pathway in *Helicobacter pylori*. *Arch. Biochem. Biophys.* **312**:349–356.
- Menz, G. L., S. L. Hazell, and B. P. Burns. 1993. Glucose utilization and lactate production by *Helicobacter pylori*. *J. Gen. Microbiol.* **139**:3023–3028.
- Menz, G. L., S. L. Hazell, and L. van Gorkom. 1994. Pyruvate metabolism in *Helicobacter pylori*. *Arch. Microbiol.* **162**:187–192.
- Mobley, H. L. T., G. L. Mendz, and S. L. Hazell. 2001. *Helicobacter pylori*: physiology and genetics. ASM Press, Washington, D.C.
- Nedenskov, P. 1994. Nutritional requirements for growth of *Helicobacter pylori*. *Appl. Environ. Microbiol.* **60**:3450–3453.
- Neidhardt, F. C., J. L. Ingraham, and M. Schaechter. 1990. Physiology of the bacterial cell. Sinauer Associates, Inc., Sunderland, Mass.
- Pitson, S. M., G. L. Mendz, S. Srinivasan, and S. L. Hazell. 1999. The tricarboxylic acid cycle of *Helicobacter pylori*. *Eur. J. Biochem.* **260**:258–267.
- Reed, J. L., T. D. Vo, C. H. Schilling, and B. O. Palsson. 2003. An expanded genome-scale model of *Escherichia coli* K-12 (iJR904 GSM/GPR). *Genome Biol.* **4**:R54.1–R54.12.
- Reynolds, D. J., and C. W. Penn. 1994. Characteristics of *Helicobacter pylori* growth in a defined medium and determination of its amino acid requirements. *Microbiology* **140**:2649–2656.
- Schilling, C. H., M. W. Covert, I. Famili, G. M. Church, J. S. Edwards, and B. O. Palsson. 2002. Genome-scale metabolic model of *Helicobacter pylori* 26695. *J. Bacteriol.* **184**:4582–4593.
- Seyler, R. W., Jr., J. W. Olson, and R. J. Maier. 2001. Superoxide dismutase-deficient mutants of *Helicobacter pylori* are hypersensitive to oxidative stress and defective in host colonization. *Infect. Immun.* **69**:4034–4040.
- Skouloubris, S., J.-M. Thiberge, A. Labigne, and H. De Reuse. 1998. The *Helicobacter pylori* UreI protein is not involved in urease activity but is essential for bacterial survival in vivo. *Infect. Immun.* **66**:4517–4521.
- Stingl, K., E.-M. Uhlemann, G. Deckers-Hebestreit, R. Schmid, E. P. Bak-

- ker, and K. Altendorf. 2001. Prolonged survival and cytoplasmic pH homeostasis of *Helicobacter pylori* at pH 1. *Infect. Immun.* **69**:1178–1181.
43. Stoner, G. L., and M. A. Eisenberg. 1975. Purification and properties of 7, 8-diaminopelargonic acid aminotransferase. *J. Biol. Chem.* **250**:4029–4036.
44. Tomb, J. F., O. White, A. R. Kerlavage, R. A. Clayton, G. G. Sutton, R. D. Fleischmann, K. A. Ketchum, H. P. Klenk, S. Gill, B. A. Dougherty, K. Nelson, J. Quackenbush, L. Zhou, E. F. Kirkness, S. Peterson, B. Loftus, D. Richardson, R. Dodson, H. G. Khalak, A. Glodek, K. McKenney, L. M. Fitzgerald, N. Lee, M. D. Adams, E. K. Hickey, D. E. Berg, J. D. Gocayne, T. R. Utterback, J. D. Peterson, J. M. Kelley, M. D. Cotton, J. M. Weidman, C. Fujii, C. Bowman, L. Watthey, E. Wallin, W. S. Hayes, M. Borodovsky, P. D. Karp, H. O. Smith, C. M. Fraser, and J. C. Venter. 1997. The complete genome sequence of the gastric pathogen *Helicobacter pylori*. *Nature* **388**:539–547.
45. Varma, A., B. W. Boesch, and B. O. Palsson. 1993. Stoichiometric interpretation of *Escherichia coli* glucose catabolism under various oxygenation rates. *Appl. Environ. Microbiol.* **59**:2465–2473.
46. Varma, A., and B. O. Palsson. 1995. Parametric sensitivity of stoichiometric flux balance models applied to wild-type *Escherichia coli* metabolism. *Biotechnol. Bioeng.* **45**:69–79.
47. Vo, T. D., H. J. Greenberg, and B. O. Palsson. 2004. Reconstruction and functional characterization of the human mitochondrial metabolic network based on proteomic and biochemical data. *J. Biol. Chem.* **279**:39532–39540.
48. Waidner, B., S. Greiner, S. Odenbreit, H. Kavermann, J. Velayudhan, F. Stähler, J. Guhl, E. Bissé, A. H. M. van Vliet, S. C. Andrews, J. G. Kusters, D. J. Kelly, R. Haas, M. Kist, and S. Bereswill. 2002. Essential role of ferritin Pfr in *Helicobacter pylori* iron metabolism and gastric colonization. *Infect. Immun.* **70**:3923–3929.
49. Wanken, A. E., T. Conway, and K. A. Eaton. 2003. The Entner-Doudoroff pathway has little effect on *Helicobacter pylori* colonization of mice. *Infect. Immun.* **71**:2920–2923.
50. Worst, D. J., M. M. Gerrits, C. M. J. E. Vandenbroucke-Grauls, and J. G. Kusters. 1998. *Helicobacter pylori* *ribBA*-mediated riboflavin production is involved in iron acquisition. *J. Bacteriol.* **180**:1473–1479.